Journal of Magnetism and Magnetic Materials 321 (2009) 2129–2134

Contents lists available at ScienceDirect

Journal of Magnetism and Magnetic Materials

journal homepage: www.elsevier.com/locate/jmmm

Magnetic measurements of suspended functionalised ferromagnetic beads under DC applied fields

Luis De Los Santos V. [a,*], Justin Llandro [a], Dongwook Lee [a], Thanos Mitrelias [a], Justin J. Palfreyman [a], Thomas J. Hayward [a], Jos Cooper [a], J.A.C. Bland [a], Crispin H.W. Barnes [a], Juan L. Arroyo C. [b], Martin Lees [c]

[a] Cavendish Laboratory, University of Cambridge, J.J Thomson Avenue, Cambridge CB3 0HE, United Kingdom
[b] Facultad de Química e Ingeniería Química, Universidad Nacional Mayor de San Marcos, Avenue Venezuela S/N, Lima 1, Peru
[c] Department of Physics, University of Warwick, Coventry CV4 7AL, United Kingdom

ARTICLE INFO

Article history:
Received 20 September 2008
Received in revised form
16 December 2008
Available online 30 January 2009

PACS:
76.60.Es
75.80.+q
85.75.−d
75.50.−y

Keywords:
Magnetic hysteresis
Magnetoelectric effect
Magnetoelectronic
Magnetic material

ABSTRACT

In this work, a simple technique to obtain the hysteresis loops of magnetic beads (Spherotech Inc.) in liquid suspension is presented. The magnetic measurements were taken in a DC Magnetic Property Measurement System (MPMS-SQUID sensor). Samples were based on ferromagnetic beads (surface-functionalized NH_2, mean diameter 4.32 μm) prepared in three conditions: dry, suspended in sucrose solution and in suspension after functionalization with fluorophore. Special small containers (1.3 cm long) made of non magnetic plastic were designed to hold the beads in liquid. The results indicate that the bead's remnant magnetization is half of the value at maximum applied field in all cases. However, due to the additional degrees of rotational freedom, beads suspended in a liquid do not present coercivity. The use of ferromagnetic beads and magnetic elements of different architectures for applications in bioassays is also discussed.

1. Introduction

The use of magnetic beads is of current interest in technology and especially in biological-related research and biotechnological applications. Particles are used in new colloidal suspensions called electrorheological fluids, which respond to an applied electric field by rapidly changing their apparent viscosity [1,2]. Particles functionalised with a variety of biochemical moieties such as antibodies, proteins or oligonucleotides are also employed in the areas of medical research and biological analysis. In addition, flow cytometry has revolutionized biological assay methods by making it possible to sort and separate literally millions of microscopic objects in minutes. Another important role of magnetic particles is their use in magnetic biosensors for labelling and screening biomolecules. A novel method for performing high throughput bioassays using digital magnetic tags that can be functionalised with various probe molecules has recently been proposed and is under development in our group [3]. The method is based on the concept of using the magnetic properties (moment, magnetization direction) of specially designed tags for encoding information (code) related to the identity of the probe molecules attached to the surface of the tags. The tags can be used in a bioassay and reveal the identity of target molecules that hybridise to the probes [4]. One implementation of magnetic encoding necessitates the use of magnetic beads, whereby target biomolecules are screened according to the moment of the beads they are attached to. A novel scheme utilizing Magnetic Avalanche Digital Detectors (MADDs) has recently been reported [5], in which individual suspended beads are detected by the effect of their stray field on the reversal processes of electrically contacted pseudo-spin valve rings. Most of these applications necessitate the use of particles suspended in solutions. For the MADD device, knowledge of the behaviour of the magnetic particles suspended in a fluid and placed under externally applied fields is important, because beads with a high moment and a large susceptibility are desired.

Despite the fact that the behaviour of magnetic particles in fluids can be deduced by means of particle fluid-dynamics, electrophoresis and magnetophoresis theory, few experimental studies can be found in the literature. Most theoretical formulas are obtained for particles in the size range from approximately 1 μm to 1 mm because the mechanics of submicron particles are strongly influenced by random thermal (Brownian) motions and

* Corresponding author. Tel.: +44 1223 337006; fax: +44 1223 337200.
E-mail addresses: luisitodv@yahoo.es, ld301@cam.ac.uk (L. De Los Santos V.).

0304-8853/$ - see front matter Crown Copyright © 2009 Published by Elsevier B.V. All rights reserved.
doi:10.1016/j.jmmm.2009.01.019

Van der Waals forces. The upper limit (10^{-3} m) is based on a reasonable working definition of what constitutes a classical particle [6,7]. The two main forces acting over a classical particle suspended in liquid medium are the gravitational force (F_G) and the buoyancy force (F_B), which cancel each other in opposite directions at equilibrium

$$F_G = \frac{\rho_p \pi d_p^3 g}{6} \tag{1}$$

$$F_B = \rho_a \frac{\pi d_p^3}{6} g \tag{2}$$

where ρ_p and ρ_a are the densities of the particle and the fluid, respectively, d_p is the diameter of the particle and g the gravity constant. When an external magnetic field is applied to a particle, a force called 'magnetophoretical' (F_M) appears, and according to [6]

$$F_M = 2\pi\mu_1 r^3 \left(\frac{\mu_2 - \mu_1}{\mu_2 + 2\mu_1}\right) \nabla H^2 \tag{3}$$

where μ_1 and μ_2 are the magnetic permeabilities of the fluid and the particle, respectively, H the external applied field and r the radius of the particle. In addition a drag force F_D appears every time the particle changes position

$$F_D = \frac{\pi d_p^2 \rho_a v^2 C_D}{8} \tag{4}$$

where C_D is the drag coefficient ($\sim$24/Re, where Re is the Reynolds number. Since the regime for microfluids is laminar, Re$<$2.0 [8]).

Measuring hysteresis loops of magnetic particles suspended in fluids is rarely reported in the literature. In most studies hysteresis loops are indirectly derived from AC susceptibility measurements [9–13]. The principal reason is the lack of equipment suitable for this task, although some researchers have designed their own instruments to measure susceptibility as a function of H (e.g. toroidal technique designed by Fannin [14]).

In this work, magnetic measurements of ferromagnetic beads in liquid suspension are performed with a classic Magnetic Property Measurement System (MPMS) Quantum Design. To achieve such measurements special holders for liquid samples were designed. The initial purpose of these measurements was to investigate the compatibility of the ferromagnetic beads with MADD biosensor designs. Specifically, knowledge regarding the possibility of switching ferromagnetic beads using the small magnetic fields generated by the electric currents flowing through MADD sensors was desired [15]. Comparisons between the M–H loops of dried beads and beads held in suspension were expected to show whether the magnetic switching of suspended ferromagnetic switching of suspended ferromagnetic beads is dominated by physical rotation of the beads, or the alteration of their internal magnetic structure.

2. Experimental

Amine-functionalized ferromagnetic beads (Spherotech Inc.) with mean diameter 4.32 μm (see Table 1) were dried, suspended in deionized (DI) water or functionalized with 5 (6)-carboxy-tetramethylrhodamine (5-(6)-TAMRA). Functionalization of samples was achieved following the procedure described in [16]. Fig. 1 shows a fluorescent microscopy image showing the TAMRA-labelled beads.

The beads were separated from water using either a centrifuge or magnetic separation. The former case required 13.2 rpm during 6 min whereas the latter is achieved by simply placing the bead solution in the vicinity of a magnetic field. After separating the beads from the water, they were dried in an oven at 35 °C overnight. In some cases it was better to evaporate the remaining water from the beads in a vacuum bell (around 10^{-1} mbar).

Preparation of samples consisting of beads in suspension was more elaborate. The density of DI water is too low to hold beads in suspension over long timescales (4–6 h are required to acquire data from the magnetometer). To avoid sedimentation, the beads were suspended in a 30% w/v and 40% w/v sucrose solution, which were prepared by dilution of 3 g (4 g) sucrose (Sigma Ultra 99.55GC) in 7 and 6 ml of DI water, respectively. These solutions were labelled as 3 × sugar and 4 × sugar, respectively.

Since the standard holder for the magnetometer consists of a simple gelatine capsule designed specially for powder and dried samples, a new holder for the solution containing the beads was designed. The equipment used for the magnetic measurements was a DC Magnetic Property Measurement System with SQUID (Quantum Design). The encapsulated sample is placed in a plastic tube and then slid down into the SQUID which is a low-pressure environment. There are two risks at this point. Firstly, the capsule begins to dissolve on contact with the liquid sample. Secondly the low pressure in the SQUID equipment could induce evaporation, and in this way not only the samples are lost, but also the equipment could suffer serious damage.

The new sample holder consisted of diamagnetic truncated cone made of plastic, 13 mm long (Fig. 2). A drop of approximately 1 μL of suspended beads in sucrose solution with a concentration of about 1.0% w/v, filled it. The ends were sealed with mounting wax. The new container was robust enough to support a pressure

Table 1
Characteristics of ferromagnetic beads for DC SQUID measurements.

Cat no.	Chemistry	Mean diameter	Amount beads/mL
AFM4010	NH_2	4.32 μm	2.3×10^8

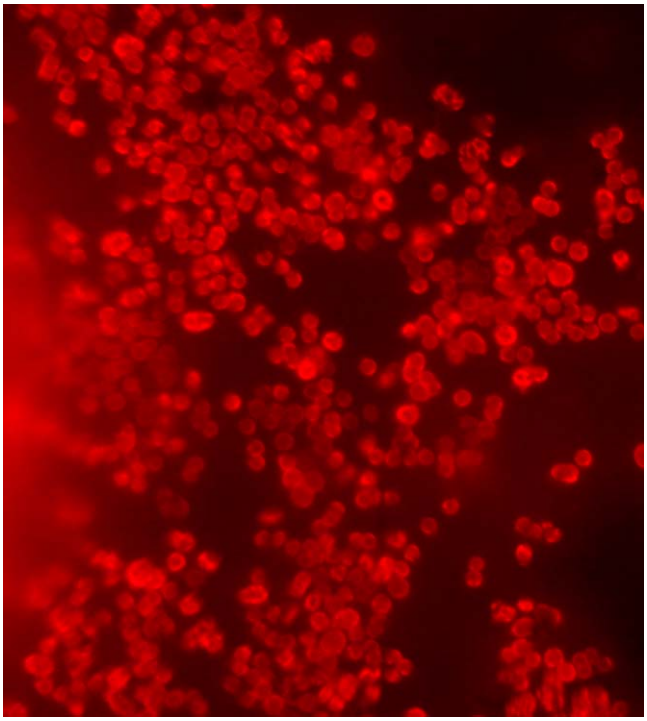

Fig. 1. Fluorescent microscopy image of 4.32 μm TAMRA-labelled ferromagnetic beads.

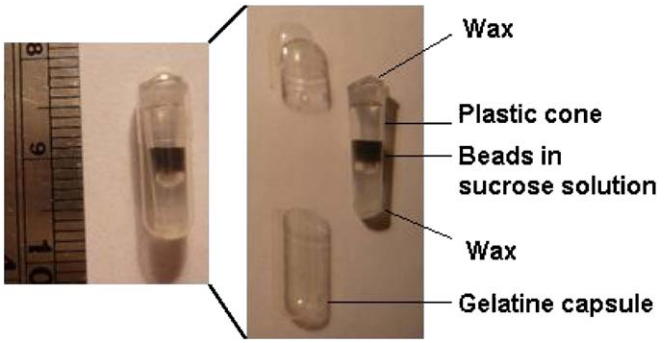

Fig. 2. Specially designed sample holders for measuring samples of suspended beads in a SQUID magnetometer. Note that there is no precipitation in the dark-coloured solution.

of 10^{-5} mbar in a previous test performed in a thermal evaporator (BOC Edwards 306).

3. Results and discussion

The hysteresis data of the ferromagnetic beads were taken in three conditions: dry, suspended and functionalized suspended. Fig. 3 shows the hysteresis loops of the dry samples. Fig. 3(a) shows the hysteresis loops at 285, 250 and 200 K under a maximum applied field of 4 kOe. Here it is noticeable that in both cases, the remnant point is always half the value of the magnetization at maximum applied field. The normalization in the M-axis was taken from $M/M_{4\,\mathrm{kOe}}$. Fig. 3(b) shows the measurements taken at five different temperatures. Despite the fact that classic hysteresis loops of ferromagnetic materials are observed, the maximum saturation has not been reached at 15 kOe. As in the previous case, the remnant magnetizations were nearly half of their maximum value in 15 kOe. As the temperature decreases, the remnant magnetic moment increases and a slight increment of the coercivity is observed. From these loops and Table 1, it is possible to obtain the magnetic moment of individual beads. Since 0.5 mL of the beads/DI water solution contains 1.15×10^8 beads, and the saturation magnetization is around 0.1 emu (for $T = 285$ K), then the magnetic moment of each individual bead is around $0.1/1.15 \times 10^8 = 8.69 \times 10^{-10}$ emu. This value is higher than for superparamagnetic beads (approximately 10^{-11} emu) and meaning that ferromagnetic beads may be more easily manipulated and detected [17].

Fig. 4 shows the hysteresis loops of the NH_2 beads (4.32 μm mean diameter) in suspension. In all cases the corresponding dry measurements under the same conditions are also shown for comparison. The magnetization axes are normalized with respect to the maximum magnetizations. The scattered points are noise caused by the motion of the beads. This noise is much less when the temperature decreases. As in the dry case the coercivity increases as the temperature decreases, however saturation is reached at around 4 kOe. At this point, it is assumed that most of the beads are aligned with the external field and then the diamagnetic behaviour of the sample holder is observed. The first two plots in the figure correspond to the beads suspended in a sucrose solution. The maximum applied field in Fig. 4(a) and (b) was 4 kOe and the measurements were taken at 285 K (a), 250 and 200 K, respectively (b). At 285 K no coercivity field was found, whereas at 250 and 200 K coercivity fields of around 900 Oe are observed. As in the dry case, the remnant moment was nearly half the maximum magnetization achieved at 4 kOe. Fig. 4(c) and (d) show the hysteresis loops also measured from beads suspended in the sucrose solution. The maximum applied field this time was

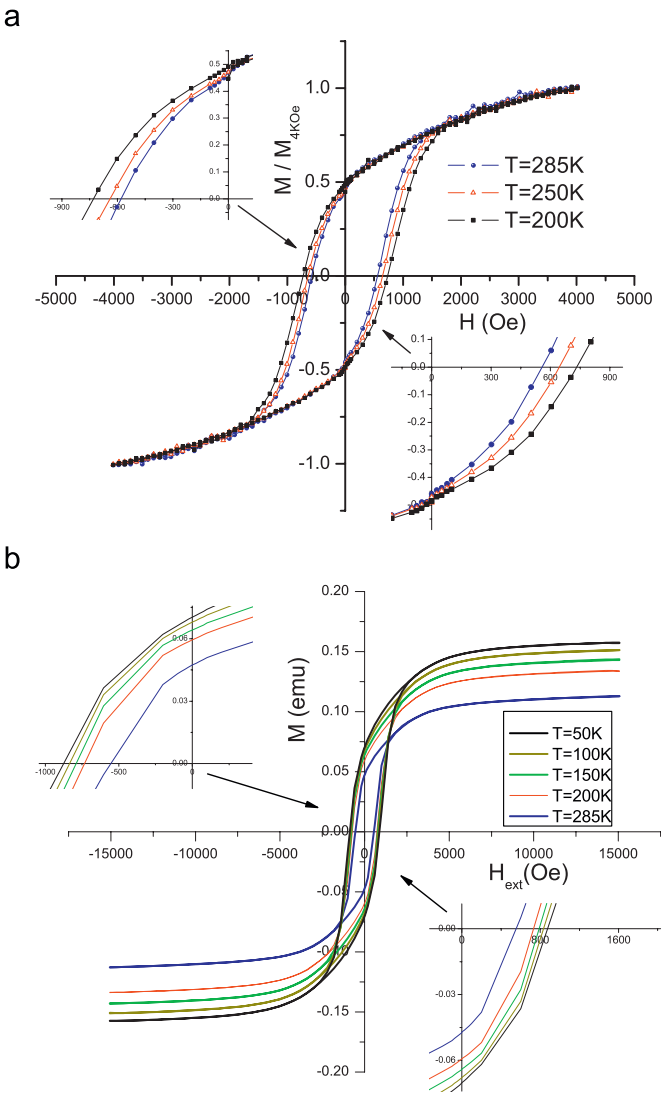

Fig. 3. Hysteresis loops for the dry NH_2 beads at different temperatures under 4 kOe maximum applied field (a) and 15 kOe maximum applied field (b).

15 kOe. The measurements were taken at five different temperatures (c) 285 K and (d) 200, 150, 100 and 50 K. When the beads reach their maximum saturation (around 4 kOe) and their magnetic moment remains constant, the diamagnetic behaviour of the plastic sample holder is noticeable, giving and downward trend in the plots. Fig. 4(e) and (f) present the hysteresis loops of TAMRA-functionalized beads suspended in phosphate buffered saline (PBS) solution. The maximum applied field was 4 kOe and the temperatures were 285 K (e), 250 and 200 K (f). The behaviour of the magnetization is the same as in the previous case.

In general, from Fig. 4 it is noticeable that near room temperature (285 K) there is no coercive field; this means that the magnetic moments of the suspended beads abruptly switch to align with the applied field when it reverses. In addition, it can be observed that, at room temperature, in the suspended case, there is a remnant magnetization in each sample; at this point some of the beads are in suspension and still aligned in the direction of the previous magnetic field. In each case, this remnant magnetization is nearly half of the maximum magnetization value which is similar to the dry case.

The M–H loop of the sample containing suspended beads can be understood as follows: since the beads are suspended in a liquid medium they have more degrees of freedom (translation

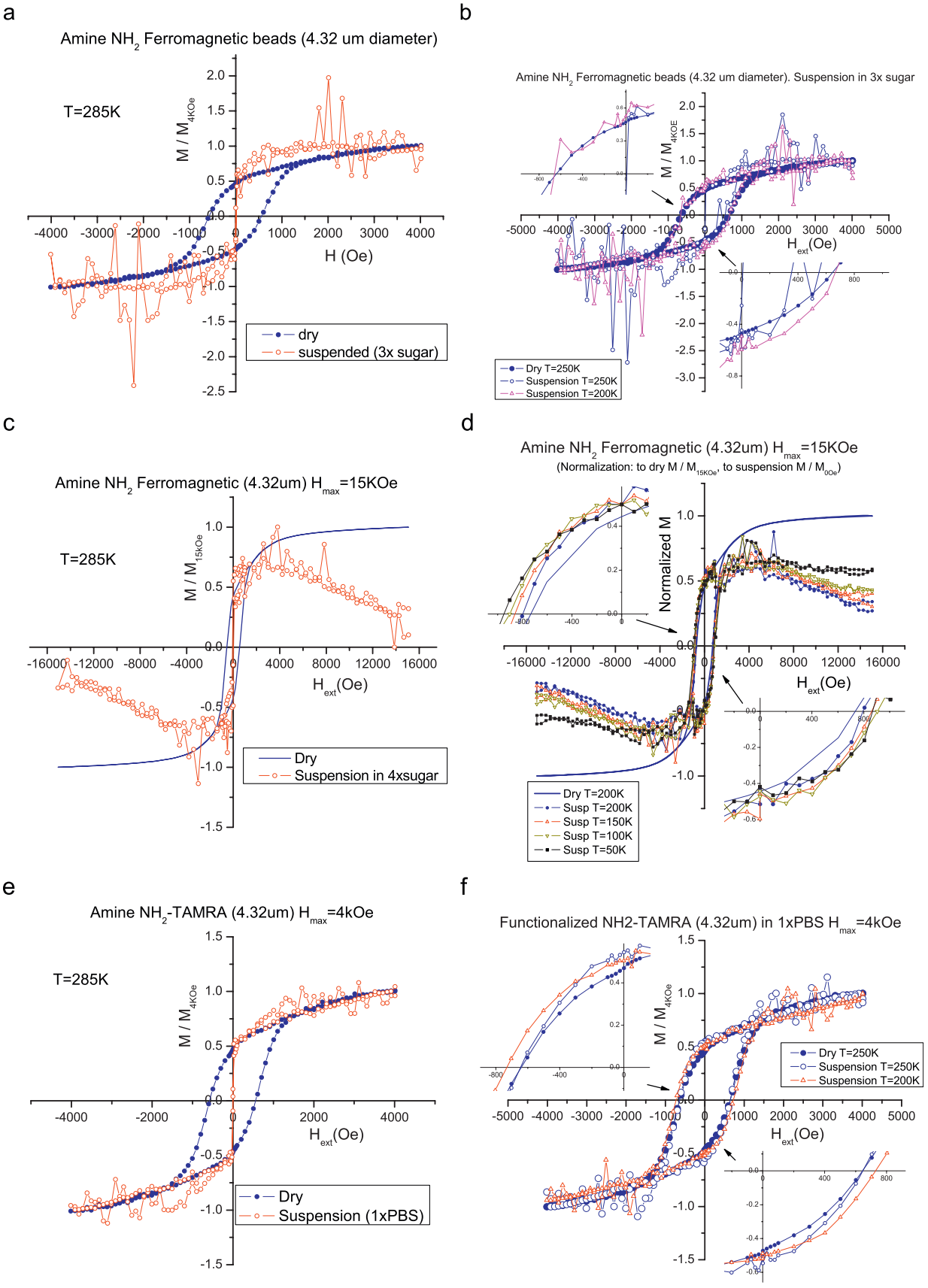

Fig. 4. Hysteresis loops of ferromagnetic beads in suspension at different temperatures. Hysteresis loops for the dry case is also plotted in each case for comparison. Note that near room temperature (285 K) no coercivity appears.

and rotation) than their dried-packed counterparts. When the external field reverses direction, the suspended beads physically rotate to align to it. This is essentially a reversible process and hence the M–H loop exhibits very little hysteresis and zero coercivity. In the dry sample, this is not possible for the beads to physically rotate since all the beads are packed or are stuck together and reorientation of the bead's magnetic domains is necessary. When the applied field switches the beads back to the opposite direction, it would be expected that the external field would align all the beads and hence the magnetization would easily become constant. However, complete saturation has not been reached at 4 kOe, probably because there is some sedimentation leading to beads become immobilized and unable to rotate so that they behave as in the dry case; the viscosity of the medium plays a role in this case too [18]. Moreover, since it is expected that the sucrose solution starts freezing from nearly 273 K, below that temperature the noise decreases and the coercivity increases, as mentioned above and confirmed in Fig. 4.

The noise in the suspended bead samples is caused by motion of the beads in suspension (Brownian motion is not applicable here as discussed at the beginning). The beads are not completely static because the sample holder is in continuous vertical movement, and hence the exact position of the beads in the SQUID equipment varies. Moreover, in equilibrium, the gravitational force, F_G, of a particular bead is equal to the buoyancy force, F_B (as mentioned before). The magnetophoretical force, F_M, generated during application of the magnetic field over the ferromagnetic bead is compensated by the drag force (F_D). The diagram of forces acting over a single bead of the sample at any arbitrary time is represented in Fig. 5. When H changes value in the MPMS, it is not uniform and F_M appears (Eq. (3)) and the beads move slightly over the applied field direction, resulting in a change of the exact position of the bead in the SQUID detection and hence the noise is produced. The vertical movement of the bead due to this change of H causes F_D (Eq. (4)). This force tries to minimize the bead displacement. As the beads accelerate, the drag force increases, causing a decrease in the acceleration. Eventually a force balance is achieved when the acceleration is zero and the maximum or terminal relative velocity is reached or when H becomes constant in the MPMS equipment. At this point not all the beads return to their original position.

In addition to the above mentioned forces, dipole–dipole interactions exist between neighboring beads. However, these interactions are always attractive and relatively short-ranged; they decay with inter-particle distances as $\sim l^{-3}$, where l is the distance between the beads [19]. Due to these forces some beads are stuck to others, forming groups. This reduces the beads degrees of freedom and the samples remnant magnetization because these groups will favor flux closure. Finally, as the temperature decreases the liquid medium freezes and the degree of freedom for the beads become limited. Therefore, switching must again occur via the reorientation of magnetic domains rather than by physical rotation, leading to non-zero coercivity. This field is expected to be nearly the same as in the dry case when the sample is completely frozen.

Fig. 6 shows the experimental detection of similarly sized (4.4 μm diameter) superparamagnetic beads (like those traditionally used in magnetic bioassay applications) using the MADD sensor. The detection geometry is shown schematically in Fig. 6(a), in which the bead is placed over a size-matched pseudo-spin valve ring in an applied field. The induced moment of the bead generates a dipole field which screens the applied field over the ring by fraction proportional to the bead moment. The success of this method for lab-on-chip applications relies on the bead moment being aligned effectively by low applied fields. Fig. 6(b) shows the effect of a 4.4 μm Dynabead® (Invitrogen) on an electrically contact pseudo-spin valve ring with a diameter of 4 μm, a linewidth of 300 nm and a layer structure of NiFe (5 nm)/Cu (4 nm)/Co (9 nm). Black solid squares and open triangles show minor magnetoresistance loops taken in the absence and presence of the bead, respectively, and clearly demonstrate that the transitions of the sensor between high and low resistance states are shifted to higher fields by approximately

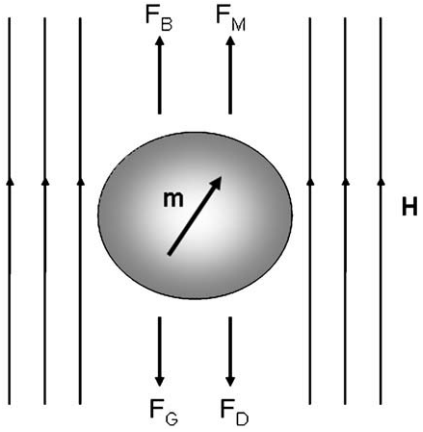

Fig. 5. Representation of the acting forces over a bead. The MPMS takes some seconds increasing or decreasing H, F_M appears during that time interval.

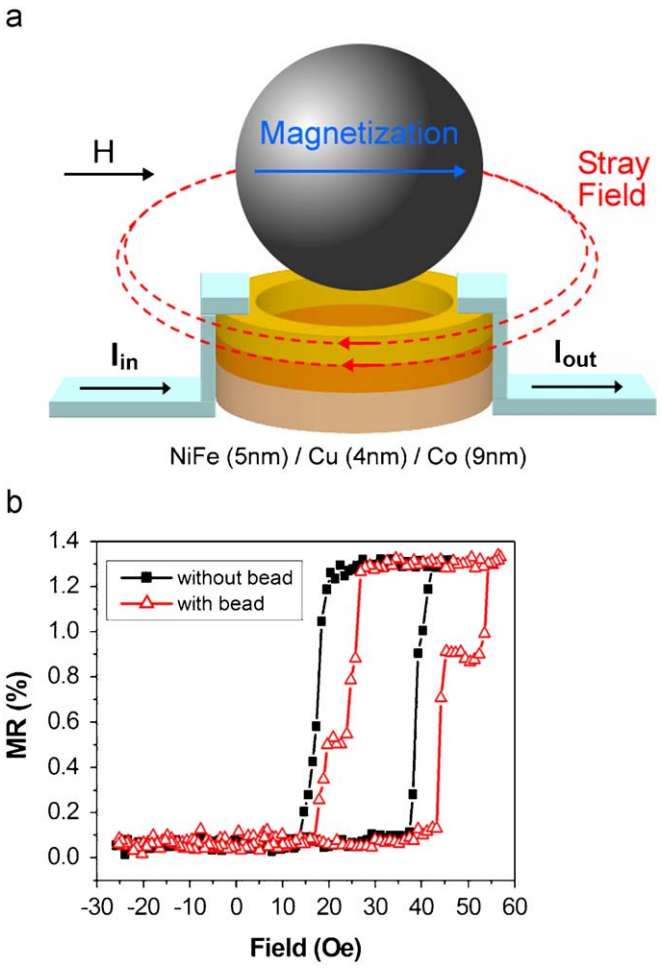

Fig. 6. (a) Schematic of bead detection using MADD sensor. (b) Minor magnetoresistance loops showing bead-induced shift in transitions of MADD sensor.

11% in the presence of a single bead of that particular moment. This data demonstrate that the experimental detection of magnetic beads with the MADD device is feasible, even if the beads are superparamagnetic and have a relatively low magnetic moment. The measurements of the magnetic moments of ferromagnetic beads presented above, indicate that a device utilizing MADD sensors and ferromagnetic instead of superparamagnetic beads will work even better.

It is also interesting to note that while the magnetic moments of the ferromagnetic beads are higher than the moments of the superparamagnetic beads that have been traditionally used in biological applications, any magnetic encoding scheme that relies on the use of different moments suffers from fundamental limitations due to the unavailability of monodisperse beads and beads with precisely controlled moments. We are exploring alternative architectures to beads in the form of electrodeposited magnetic micropillars, nanowires and planar magnetic structures that can be utilized as magnetic tags for biological applications. Because the pillars are made of solid magnetic material, these structures give a much larger magnetic signal than the magnetic beads [20,21]. The use of micropillars as magnetic tags could, therefore, be very promising since they can be manipulated more easily by means of local magnetic fields applied by tapered current striplines on the surface of a lab-on-chip device, as well as being easier to detect with magnetic sensors. In addition, the natural encoding ability of the magnetic elements can be utilized by combining different magnetic layers into a single micropillar so that a magnetic tag can be designed, such that the direction of magnitude of the magnetization of each layer can correspond to a digital code [20].

4. Conclusions

A method of measuring the hysteresis loops of magnetic microbeads held in suspension has been demonstrated. The measurements of the magnetic moment of individual NH_2 beads (4.32 μm mean diameter), obtained by dividing the maximum saturation between the amounts of particles, was around 8.69×10^{-10} emu at room temperature. The remnant magnetization is nearly half of this value for all the samples including those that are held in suspension and functionalized. However, due to the extra degrees of freedom of beads suspended in a liquid, such samples have zero coercivity, whereas dry samples exhibit a coercivity of several hundred Oesters. When the external applied fields change direction, the suspended beads can rapidly rotate to align their internal magnetic structure. When the temperature of the suspended bead samples decreases freezing the liquid medium, a non-zero coercivity appears. Such behaviour lets us to conclude that the magnetization not only depends on subdomains such as in the dry case, also the physical rotations of the beads play a role. The fact that freely suspended ferromagnetic beads will abruptly reverse their magnetic orientation by rotation has implications for any magnetic beads sensing method which depends on proximity detection of the beads by an embedded sensor. It is likely that the beads follow changing field directions from AC sensor currents; at least at low frequencies which is important for magnetic assay methods which attempt to measure beads in flow. Assay methods involving the immobilization of beads may be also able to take advantage of the change in coercivity generated by the loss of rotational degrees of freedom as the beads bind to the sensor surface.

Acknowledgements

Luis De Los Santos thanks the European Union Programme of High Level Scholarships for Latin America (ALBAN Scholarship no. E06D101257PE) and the Cambridge Overseas Trust (COT bursary) for financing his Ph.D studies.

References

[1] Yuji Hirose, Yasufumi Otsubo, Colloids Surf. Eng. Aspects 317 (2008) 438.
[2] T. Belza, et al., Physica A 385 (2007) 1.
[3] T. Mitrelias, T. Trypiniotis, F. van Belle, K.P. Kopper, S.J. Steinmuller, J.A.C. Bland, P.A. Robertson, in: Conference Proceedings Series of the American Institute of Physics, vol. 1025, 2008, pp. 60–73.
[4] B. Hong, J.R. Jeong, J. Llandro, T.J. Hayward, A. Ionescu, T. Mitrelias, K.P. Kopper, S.J. Steinmuller, T. Trypiniotis, J.A.C. Bland, in: Conference Proceedings Series of the American Institute of Physics, vol. 1025, 2008, pp. 74–81.
[5] J. Llandro, T.J. Hayward, D. Morecroft, J.A.C. Bland, F.J. Castaño, I.A. Colin, C.A. Ross, Appl. Phys. Lett. 91 (2007) 203904.
[6] Y. Thomas, B. Jones, Electromechanics of Particles, Cambridge University Press, Cambridge, 1995.
[7] P.C. Fannin, et al., J. Magn. Magn. Mater. 303 (2006) 147.
[8] Carl Hansen, Kaston Leung, Payam Mousavi, Phys. World 20 (9) (2007) 24.
[9] P.C. Fannin, S.W. Charles, J. Magn. Magn. Mater. 196–197 (1999) 586.
[10] A. Prieto-Astalan, F. Ahrentop, C. Johanson, K. Larson, A. Krozer, Biosens. Bioelectron. 19 (2004) 945.
[11] R. Kötzitz, W. Weitschies, L. Trahms, W. Brewer, W. Semmler, J. Magn. Magn. Mater. 194 (1999) 62.
[12] P.C. Fannin, et al., J. Magn. Magn. Mater. 201 (1999) 91.
[13] S.H. Chung, A. Hoffman, S.D. Bader, C. Liu, B. Kay, L. Makowski, L. Chen, Appl. Phys. Lett. 95 (2004) 2971.
[14] P.C. Fannin, J. Phys. E: Sci. Instrum. 19 (1986) 238.
[15] L. Ejsing, M.F. Hansen, A.K. Menon, H.A. Ferreira, D.L. Graham, P.P. Freitas, J. Magn. Magn. Mater. 293 (2005) 677.
[16] T. Mitrelias, J. Palfreyman, Z. Jiang, J. Llandro, J.A.C. Bland, R.M. Sanchez-Martin, M. Bradley, J. Magn. Magn. Mater. 310 (2007) 2862.
[17] Z. Jiang, J. Llandro, T. Mitrelias, J.A.C. Bland, J. Appl. Phys. 99 (8) (2006) 08S105.
[18] T.M. Kwon, M.S. Jhon, H.J. Choic, J. Mol. Liq. 75 (1998) 115.
[19] Karolina Peterson, Dag Ilver, Christer Johanson, Anatol Krozer, An. Chim. Act. 573–574 (2006) 138.
[20] J. Palfreyman, F. van Belle, W.S. Lew, T. Mitrelias, J.A.C. Bland, M. Lopalco, M. Bradley, IEEE Trans. Magn. 46 (6) (2007) 2439.
[21] F. van Belle, J. Palfreyman, W.S. Lew, T. Mitrelias, J.A.C. Bland, In: Conference Proceedings Series of the American Institute of Physics, vol. 1025, 2008, pp. 34–43.